

§32. Observed Pressure Gradients at a Peripheral Rational Surface in LHD High Beta Plasma

Watanabe, K.Y., Sakakibara, S., Narushima, Y.

Ideal MHD instabilities have a possibility to strongly limit the operational regime of the plasma parameters such as beta, pressure gradient and/or so on. In tokamaks, it is well known that the operational beta limits are quite consistent with theoretical predictions of ideal linear MHD theory. On the contrary, in helical plasmas, a limited number of systematic studies about the effect of pressure driven ideal MHD instabilities on the operational beta range in experiments have been reported. In order to study the role of low mode number ideal pressure driven MHD modes on the operational beta range in LHD, we compare between the experimentally observed pressure gradients at peripherally located resonant rational surfaces and the theoretically predicted unstable region for ideal pressure driven MHD instabilities in the new high aspect configuration with $R_{ax}=3.6m/A_p=6.3$, where the achieved beta value has been extended to 4%.

Figure 1 shows observed beta gradients and contours of the growth rate of low-n ideal MHD mode with a global mode structure in the $\langle\beta\rangle$ - $d\beta/d\rho$ diagram in a peripheral low order rational surface ($\rho=0.9$, $\iota\sim 1$). Here ρ and ι are a normalized minor radius and a rotational transform, respectively. Solid and dotted lines denote contours of the low-n ($m/n=1/1$) ideal MHD modes (with global mode structure) with $\gamma_{low-n}/\omega_A=10^{-2}$ and 3×10^{-3} for currentless equilibria. The growth rate is calculated with a MHD stability analyzing code (TERPSICHORE). Here $\omega_A=v_{A0}/R_0$, v_{A0} and R_0 are the Alfvén velocity and the major radius at the magnetic axis. The dashed lines are the stability boundary of Mercier modes (with a highly localized mode structure / high-m limit), which corresponds to the $\gamma_{low-n}/\omega_A=0$ contour of the low-n mode. Figures 2 (a) and (b) show the mode structures of the ideal MHD unstable mode at the symbols, "a" and "b" in Fig.1, respectively. Here we are considering a fixed boundary mode. Both eigenfunctions are dominated by an almost single mode. From Figs 1 and 2, the mode width of the MHD unstable modes with $\gamma_{low-n}/\omega_A=10^{-2}$ and 3×10^{-3} are $\sim 5\%$ and $\sim 1\%$ of the plasma minor radius, respectively. The mode width is quite narrower than that of the MHD unstable mode resonant with the core low-n rational surface, for example, $m/n=2/1$ because the magnetic shear is stronger than that in the core region. The circle symbols in Fig.1 correspond to the observed thermal beta gradients, which is estimated based on measured electron temperature profile and density profile. Here $Z_{eff}=1$ and $T_i=T_e$ are assumed. The data were obtained in 0.45T to 1.75T operation. The envelope of the observed beta gradients at $\rho=0.9$ increases with the beta up to $\langle\beta_{dia}\rangle=4\%$. Though a change of the envelope is observed around $\langle\beta_{dia}\rangle=1.5\%$ which corresponds to the Mercier unstable region, clear boundary is not observed up to $\langle\beta_{dia}\rangle=4\%$. The envelope of the observed thermal pressure gradients in the

beta range of $\langle\beta_{dia}\rangle=3-4\%$ corresponds to coincide with a contour of the $m/n=1/1$ ideal MHD mode with $\sim 5\%$ of the plasma minor radius as the mode width.

Figure 3 shows the radial profile of the growth rate of the high-n ideal ballooning modes at the symbols "a" in Fig.1. At $\langle\beta_{dia}\rangle\sim 4\%$, the high-n ballooning mode is as unstable as the low-n interchange mode. The systematic analysis of the relationship between the ballooning modes and experiments is a future subject of exploration.

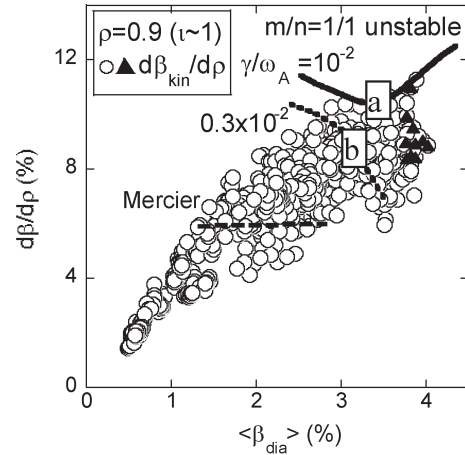


Fig.1 The contours of low-n ideal MHD mode growth rate calculated in $\langle\beta\rangle$ - $d\beta/d\rho$ diagram.

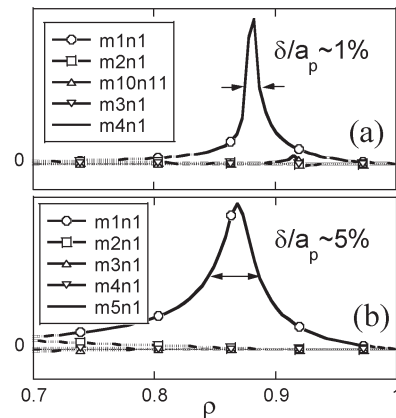


Fig.2 The eigenfunction profiles of the low-n ideal MHD unstable mode for (a) "a" and (b) "b" in Fig.1

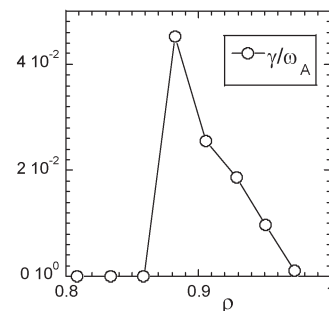


Fig.3 The normalized growth rate profiles of the high-n ballooning mode for the pressure profile corresponding to the point of "a" in Fig.1.